

Collage Prompting: Budget-Friendly Visual Recognition with GPT-4V

Siyu Xu¹, Yunke Wang², Daochang Liu¹, and Chang Xu¹

¹ School of Computer Science, The University of Sydney
`{s.xu, daochang.liu, c.xu}@sydney.edu.au`

² School of Computer Science, Wuhan University
`yunke.wang@whu.edu.cn`

Abstract. Recent advancements in generative AI have suggested that by taking visual prompt, GPT-4V can demonstrate significant proficiency in image recognition task. Despite its impressive capabilities, the financial cost associated with GPT-4V’s inference presents a substantial barrier for its wide use. To address this challenge, our work introduces Collage Prompting, a budget-friendly prompting approach that concatenates multiple images into a single visual input. With collage prompt, GPT-4V is able to perform image recognition on several images simultaneously. Based on the observation that the accuracy of GPT-4V’s image recognition varies significantly with the order of images within the collage prompt, our method further learns to optimize the arrangement of images for maximum recognition accuracy. A graph predictor is trained to indicate the accuracy of each collage prompt, then we propose an optimization method to navigate the search space of possible image arrangements. Experiment results across various datasets demonstrate the cost-efficiency score of collage prompt is much larger than standard prompt. Additionally, collage prompt with learned arrangement achieves clearly better accuracy than collage prompt with random arrangement in GPT-4V’s visual recognition.

Keywords: GPT-4V · Large Language Models · Efficient Inference

1 Introduction

With the rapid development of generative AI, various large language models (LLMs) [4, 29, 45] have emerged as generative tools. Beyond text, these models have expanded their capabilities to include text-to-image generation such as Stable Diffusion [25], and text-to-video generation, as seen in Sora [21]. ChatGPT [3], as the most well-known LLMs, has shown it can have natural and coherent conversations, making it a powerful tool in daily life and different industry fields. As the latest version of ChatGPT, GPT-4V is a multi-modal LLM capable of processing both text and images. This capability allows it to be applied to a wider range of applications and tasks. There are many technical reports and user studies [16, 17, 27, 35, 41, 47] about GPT-4V, which conducted thorough evaluations of its capabilities from various aspects.

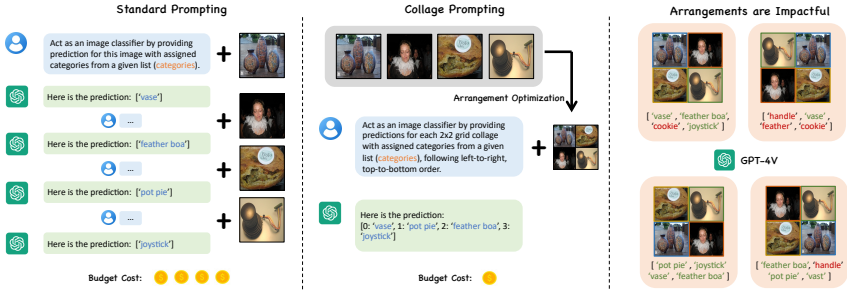


Fig. 1: Visual recognition of GPT-4V with different prompting ways. (a): **Standard prompting** takes one image as visual prompt for each GPT-4V’s run. (b): **Collage prompting** concatenates multiple images into one visual prompt and predicts class for all images in each inference. (c): The arrangement of images within collage prompting leads to significantly different results. **Green** indicates an accurate prediction while **red** indicates an wrong prediction.

In [38], the visual capabilities of GPT-4V are investigated within the framework of zero-shot visual recognition tasks, such as image and video recognition. The evaluation of visual capabilities is quite straightforward: images and candidate categories are directly fed into GPT-4V for relevance ranking, yielding Top-1 and Top-5 prediction results. Video and point cloud data are uniformly sampled to generate a set of images, which are then processed by GPT-4V for visual recognition. GPT-4V has achieved remarkable performance across various visual recognition tasks, surpassing previous customized solutions [10, 34]. However, its financial cost associated with its inference can be significant. Specifically, performing image recognition on the ImageNet-1K dataset [26] requires approximately \$1 for every 20 images, leading to a total evaluation cost of over \$2,500 for the entire dataset. If we consider the rate limit of maximum API requests per minute, the costs will be even higher. Thus, employing GPT-4V for visual recognition tasks is expensive, and it is meaningful to adopt a more budget-friendly way for GPT-4V’s visual recognition.

In GPT-4V’s visual recognition, it takes only a single image as the visual prompt. This standard prompting way fails to fully release the potential capacity of GPT-4V, which is able to process multiple inquiries within one prompt simultaneously. Motivated by this idea, we propose **Collage Prompting**, a new visual prompting way for GPT-4V’s visual recognition for budget-friendly inference. In collage prompt, multiple images are collaged into one visual prompt with equal size. GPT-4V is then requested for recognizing the class for all images within this prompt. The overall process is shown in Figure 1b. Since collage prompting way allows for the recognition of multiple images in one run of GPT-4V, it significantly reduces the overall cost. Furthermore, based on the observation in Figure 1c that different arrangements of images within collage prompt could lead to rather large variance of accuracy in GPT-4V’s recognition,

we propose to **Learn to Collage Prompt (LCP)** based on the idea of genetic algorithm. The collage prompt is represented as a graph and a collage predictor is used for estimating the expected accuracy of this collage prompt. LCP is then used for searching for the best arrangement in several iterations.

The contributions of this paper can be summarized as follows,

- We propose a budget-friendly prompting approach for GPT-4V. By involving multiple images into a single visual prompt, GPT-4V can process multiple images in an inference run, thus reducing the overall expense greatly.
- We collect the evaluation dataset of collage prompt. The datasets contain various collage prompts from the ImageNet-1K training set and their accuracy in GPT-4V’s image recognition. This dataset is meaningful for studying the effectiveness of collage prompting.
- We propose a genetic algorithm-based optimization method for collage arrangement. This approach aims to find the optimal arrangement for collage prompts and maximize accuracy in image recognition within GPT-4V.

2 Related Works

2.1 Exploration of GPT-4V

The state-of-the-art large multi-modal model GPT-4V was firstly launched at September 2023 and has demonstrated its strong visual capability in different fields. Early works [39, 41] conducted user study of GPT-4V, where operations were completed by entering prompts on a web interface for GPT-4V. Furthermore, the release of GPT-4V API in November 2023 opened up new opportunities for both academic community and industry to thoroughly evaluate GPT-4V’s performance across various visual benchmarks and provide quantitative data beyond what user studies can offer. GPT-4V’s capacities in multimodal medical diagnosis has been explored in [9, 36, 42], where GPT-4V can process different imaging modalities like CT and MRI in medical scene. GPT-4V can also be utilized to operate robots from providing instructions by taking multi-modal input in autonomous driving [8, 12, 35] and task planning [14, 31, 32]. Additionally, GPT-4V has been widely used in advancing video understanding [17], conducting OCR recognition [27], acting as an intelligent web agent [46], and dealing with each observation data [43]. [38] is the first work that considers to adopt extensive quantitative analysis utilizing the established visual benchmarks. However, the evaluation of GPT-4V on visual benchmarks could lead to large expense, since every inference made by GPT-4V will cost money. Hence, it is important to adopt a budget-friendly inference scheme for the evaluation of GPT-4V.

2.2 Prompt Engineering in LLMs

Prompt engineering has emerged as a crucial technique for unlocking the potential of pre-trained large language models (LLMs) and vision-language models

(VLMs). The concept of prompt engineering was initially explored and popularized in the LLMs [5, 18, 30] and VLMs [1, 37]. The most common prompting way is zero-shot prompting [6, 24], which offers a paradigm shift in leveraging large LLMs. This method significantly reduces the dependency on vast amounts of training data by employing strategically formulated prompts to steer the model towards executing new tasks. While the primary focus in the field has been on creating prompts that can release the potential capacities of LLMs, we focus on developing a prompting approach that prioritizes cost-efficiency.

3 Methodology

GPT-4V has enabled us to perform comprehensive visual recognition. However, each inference performed by GPT-4V incurs a financial cost, which is determined by the number and type of input and generated tokens³. Specifically, for image recognition tasks involving images of 512×512 resolution, approximately 5000 tokens are consumed per image. Standard prompting of GPT-4V involves presenting a single image as a visual prompt and processing each image in the dataset individually. With this standard prompting, the expense of evaluating a dataset with 10,000 images could exceed \$500. This prompting way is expensive, and a more budget-friendly way is to process multiple images simultaneously in a single inference run.

Motivated by this idea, we propose Collage Prompting, an efficient alternative to standard visual prompting. Collage Prompting involves concatenating multiple images into a single visual prompt, allowing for simultaneous processing in a single inference run. For example, employing a nine-grid collage prompting approach can decrease expenses to just $1/9$ of what standard individual image prompting incurs. Moreover, given that there are $9! = 362,880$ possible configurations for arranging images within a nine-grid collage prompt, identifying the optimal arrangement to maximize GPT-4V’s visual recognition accuracy becomes a crucial problem. And we aim to find the best configuration that ensures high accuracy in GPT-4V’s visual recognition tasks.

3.1 Collage Prompting

GPT-4V’s basic workflow for visual recognition involves taking visual samples as prompts and accompanying them with a textual description that enumerates the categories present in the dataset, as shown in Figure 1a. This combination of visual and text prompts enables GPT-4V to match the visual input with the correct categories. The GPT-4V model analyzes the image, categorizes it based on relevance to the provided text prompt, and predicts the class of the visual input. The effectiveness of GPT-4V in this context is often measured by its Top-1 accuracy in image recognition.

When applying GPT-4V to image recognition tasks across datasets with N visual samples using the standard prompting method, it necessitates N separate

³ <https://openai.com/pricing>

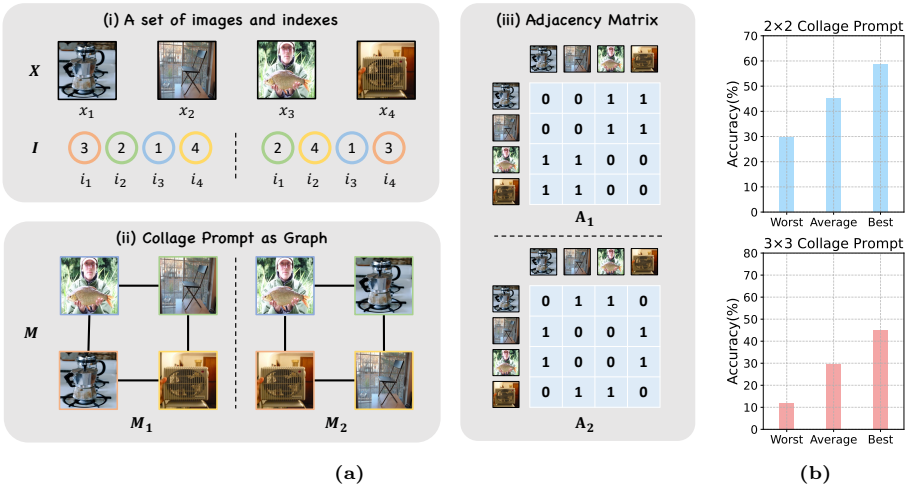


Fig. 2: (a): The workflow of forming the collage prompt from a set of images and related indexes. For a set of images \mathbf{X} with two different position indexes \mathbf{I} , we can obtain two collage prompts M_1 and M_2 . Regarding \mathbf{X} as the node of a graph, the adjacency matrix of M_1 and M_2 can be represented as A_1 and A_2 . (b): The average accuracy of collage prompts within evaluation datasets using ‘Worst’, ‘Average’ and ‘Best’ arrangement.

inferences. Considering the cost associated with each inference, the total expense of evaluating an entire dataset can be substantial. To mitigate these costs, we propose the concept of collage prompting, which allows for the evaluation of multiple visual samples within a single inference run. By assembling K images into one comprehensive visual prompt, we can significantly decrease the inference cost to $1/K$ of the standard method. The collage prompt \mathbf{M} is designed to be a $\sqrt{K} \times \sqrt{K}$ grid and each grid contains one image. For example, a collage of four images might be presented in a quadrant grid, while nine images could be arranged in a nine-grid format.

Supposing we have a set of K images $\mathbf{X} = [x_1, x_2, \dots, x_K]$ and its related position indexes $\mathbf{I} = [i_1, i_2, \dots, i_K]$, where i_j indicates the position number of image x_j in the collage prompt, starting from 0 in the top left corner to $K - 1$ in the bottom right corner. Hence, the row position r and column position c of image x_j can be specified as $r = \lfloor (i_j - 1) / \sqrt{K} \rfloor$ and $c = (i_j - 1) \bmod \sqrt{K}$ respectively. While collage prompt \mathbf{M} has the same size as the standard prompt, GPT-4V can thus take this collage prompt as input and generate the predicted class for all images within the collage prompt.

Collage Prompt as Graph. Regarding the collage prompt \mathbf{M} as graph $\mathbf{M} = (\mathbf{A}, \mathbf{F})$ with K nodes, each node $f_i \in \mathbb{R}^l$ denotes the feature of x_i , which is extracted from CLIP’s encoder [23]. The adjacency matrix $\mathbf{A} \in \mathbb{R}^{K \times K}$ suggests

the relative positions of \mathbf{X} , where two adjacent images are considered to have an undirected edge. For two images x_p and x_q that satisfies either $|c_p - c_q| = 1$ when $r_p = r_q$ or $|r_p - r_q| = 1$ when $c_p = c_q$, we consider these two images have an edge and set $\mathbf{A}[p, q] = \mathbf{A}[q, p] = 1$. The workflow of representing the collage prompt as a graph is illustrated in Figure 2a.

3.2 Arrangements Matter

To fill multiple images into the collage prompt, the arrangement of these images could be various. As shown in Figure 2a, by setting different \mathbf{I} , the arrangement of images within the collage prompt is different. Technically, a quadrant-grid collage has 24 potential image arrangements, whereas a nine-grid format can exceed 360,000 possibilities. Our findings in Figure 2b indicate that different arrangements can yield varying levels of accuracy, underscoring the importance of optimal image placement within the collage. To determine the most effective configuration for a collage prompt, we utilize a collage predictor. This predictor is designed to predict the expected accuracy of a specific collage arrangement. To facilitate this, it is necessary to first collect an evaluation dataset that contains evaluation outcomes of various collage prompt.

Evaluation Dataset. To form various collage prompt, we first uniformly sample a sub-dataset that contains 100,000 images from the training set of ImageNet-1K [26]. This subset is then divided into L groups, and each group contains K images. By executing p random shuffles of the images within each group, we generated a collection of $L \times p$ unique collage prompts. We collect two evaluation datasets with a quadrant-grid collage prompt and a nine-grid collage prompt. For the quadrant-grid collage prompt, L is set to be 25,000 and p is set to be 5. For the nine-grid collage prompt, L is set to be 11,111 and p is set to be 10. These collage prompts are then sent into GPT-4V’s API for image recognition and the accuracy y of each prompt can be obtained. The final evaluation dataset \mathcal{D} thus includes pairs $\{\mathbf{M}_i, y_i\}$ for each of the $L \times p$ prompts, providing a comprehensive basis for analyzing the effectiveness of different collage configurations in visual recognition tasks.

As stated the previous subsection, collage prompt \mathbf{M} is represented as a graph. To analyze and predict the performance of these collage prompts, we employ a Graph Convolutional Neural Network (GCN) [44], denoted as $G_\theta(\mathbf{A}, \mathbf{F})$, to process the graph data and predicts the expected accuracy of the collage prompt. For the i -th layer in $G_\theta(\mathbf{A}, \mathbf{F})$, it takes the adjacent matrix \mathbf{A} and hidden representation matrix \mathbf{H}_i as input, then the next layer’s output can be generated as follows,

$$\mathbf{H}_{i+1} = \sigma(\tilde{\mathbf{D}}^{-\frac{1}{2}} \tilde{\mathbf{A}} \tilde{\mathbf{D}}^{-\frac{1}{2}} \mathbf{H}_i \mathbf{W}^i), \quad (1)$$

where $\sigma(\cdot)$ is the non-linear activation function and $\mathbf{H}_0 = \mathbf{X}$, $\tilde{\mathbf{A}} = \mathbf{A} + \mathbf{I}$ is the adjacent matrix with self-connections. $\tilde{\mathbf{D}}$ is the diagonal degree matrix of

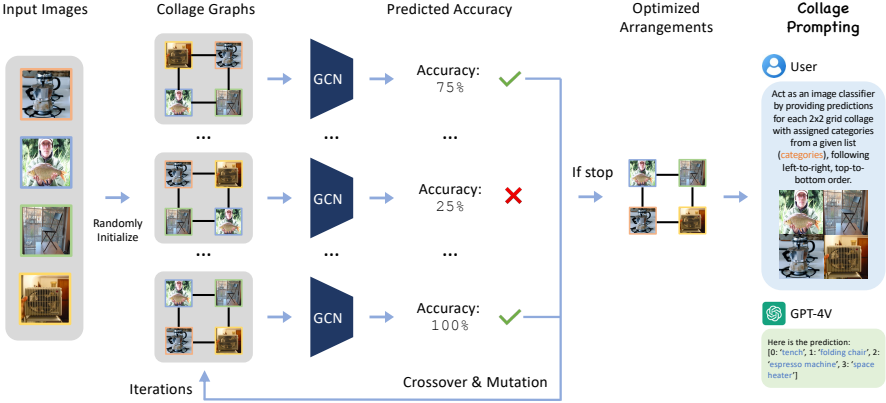


Fig. 3: An overview of proposed method LCP. Starting with a set of images, index sets are randomly initialized, which forms multiple collage graphs. After predicting the accuracy of each collage graphs via G_{θ^*} , collage graphs that achieves top- T accuracy are selected for crossover and mutation operations. This iterative process continues until reaching the maximum specified iteration, and we can obtain the optimized arrangements within the collage prompting.

$\tilde{\mathbf{A}}$, and $\mathbf{W}^i \in \mathbb{R}^{d \times d}$ is the trainable weight matrix. As the layer gets deeper, there exists graph pooling to progressively reduce the node and the remaining one node at the final layer will be sent into a MLP head to predict the accuracy. Given the evaluation dataset $\mathcal{D} = \{\mathbf{M}_i, y_i\}_{i=1}^{L \cdot P}$, the update of the $G_{\theta}(\mathbf{A}, \mathbf{F})$ at k -th iteration can be expressed as,

$$\theta_{k+1} = \theta_k - \frac{\eta}{b} \sum_{i=0}^b \nabla_{\theta} L(G_{\theta}(\mathbf{A}_i, \mathbf{F}_i), y_i), \quad (2)$$

where b is the batch size of training, η is the learning rate and L denotes the MSE loss. At the convergence step, θ^* will be obtained and \mathbf{G}_{θ^*} can be used to indicate the expected accuracy of the collage prompt \mathbf{M} .

3.3 Learning to Collage

With the trained predictor \mathbf{G}_{θ^*} , we can estimate the accuracy for various arrangements in the collage prompt, which enables the selection of the most effective arrangement to enhance recognition performance with GPT-4V. Due to the vast number of potential arrangements, it is impractical to evaluate each one to identify the optimal arrangement. To efficiently search for the best arrangement within a maximum number of iterations, we propose **Learning to Collage Prompt (LCP)** to achieve effectively searching.

Genetic algorithm has been widely used for non-differentiable optimization problems [33]. Following the framework of genetic algorithm, LCP contains sev-

Table 1: Statistics of datasets used for evaluating collage prompting.

Datasets	Classes	Samples	Label Tokens
ImageNet-1K [26]	1,000	50,000	4,834
Caltech101 [11]	100	2,465	428
OxfordPets [22]	37	3,669	203
StanfordCars [15]	106	8,041	1,814
Flowers102 [20]	102	2,463	562
Food101 [2]	101	30,300	513
FGVCAircraft [19]	100	3,333	565
SUN397 [40]	397	19,850	1,859
DTD [7]	47	1,692	211
EuroSAT [13]	10	8,100	49
UCF101 [28]	101	3,783	526

eral stages in each iteration: initialization, evaluation, selection, crossover, and mutation. In the initialization phase, for a given set of image features \mathbf{F} , we randomly generate a set of position index set $\mathcal{I} = \{\mathbf{I}_1, \mathbf{I}_2, \dots, \mathbf{I}_P\}$ with the related adjacency matrices $\mathcal{A} = \{\mathbf{A}_1, \mathbf{A}_2, \dots, \mathbf{A}_P\}$. These matrices represent different possible arrangements of the collage prompt. Subsequently, for each adjacency matrix \mathbf{A}_i in \mathcal{A} , we predict its expected accuracy using $\hat{y}_i = G_{\theta^*}(\mathbf{A}_i, \mathbf{F})$, resulting in a set of predicted accuracy $\mathcal{Y} = \{\hat{y}_0, \hat{y}_1, \dots, \hat{y}_P\}$. During the selection phase, we choose a subset $\tilde{\mathcal{I}}$ of arrangements from \mathcal{I} that correspond to the top- T accuracy in \mathcal{Y} , indicating the most promising arrangements.

To generate the next generation of arrangements, crossover and mutation operations are applied to the selected subset $\tilde{\mathcal{I}}$. Specifically, in the crossover process, the new position index $\hat{\mathbf{I}}$ is divided into several segments. Each segment is determined by the corresponding part of each position index $\mathbf{I} \in \tilde{\mathcal{I}}$. Therefore, the new position index will be the fusion of the optimal arrangements in the last iteration. In the following mutation process, a set of position indexes will be generated based on $\hat{\mathbf{I}}$. This process iteratively continues, refining the search for an arrangement that maximizes the accuracy of collage prompt recognition by GPT-4V.

4 Experiment

4.1 Datasets

We evaluate the performance of collage prompt on ImageNet-1K and 10 other common downstream image recognition datasets. Table 1 presents statistics regarding the number of test samples and label tokens for each dataset. Label tokens represent the number of tokens encoded by the GPT-4 tokenizer⁴, providing a measure of the textual labels’ complexity for each dataset.

⁴ <https://platform.openai.com/tokenizer>

Evaluation Dataset. The evaluation dataset introduced in Section 3.2 is used for training the collage predictor and is derived from the ImageNet-1K training dataset, where we randomly and uniformly selected 100,000 images across all categories to construct 2×2 and 3×3 collage prompt evaluation datasets. We collected two groups of evaluation datasets with GPT-4V. The first group is the 2×2 grid dataset, which contains 25,000 sets of 2×2 grids. Each set of 2×2 grids has approximately 5 different arrangements, resulting in 110,250 valid training data points with GPT-4V. The second group is the 3×3 grid dataset, which contains 11,111 sets of 3×3 grids. Each set of 3×3 grids has about 10 different arrangements, yielding 102,646 valid training data points with GPT-4V. We will release the evaluation dataset after the acceptance of this paper.

4.2 Implementation Details

GPT-4V API. We utilize the GPT-4V API⁵, where the image input size can be selected from low, high, and auto options. We choose to use the low resolution, which defaults to 512×512 pixels, costing only 85 tokens per image. All our images are resized to 512×512 before being input into GPT-4V, thus avoiding any further resizing. Through experimental testing and cost analysis, we find that using high resolution was not cost-effective. It only offers minimal improvements in accuracy at a cost several times higher than low resolution. We recommend using low resolution for extensive GPT-4V applications. For the text prompt in GPT-4V, we follow the design of GPT4Vis [38]. We also observe that not providing the model with category labels, and relying solely on the model’s pre-learned knowledge for prediction, could result in the prediction of non-existent categories, with inconsistent category names. However, datasets with a large number of categories consume a significant amount of tokens. For instance, the category labels of ImageNet-1K require 4,834 tokens, leaving only 211 tokens for the remaining text, while images consume just 85 tokens.

4.3 Metrics

We use **cost** (US Dollars) and **accuracy** as our primary evaluation metrics and introduce two new metrics based on these two fundamental indicators.

- **Cost-Effective Ratio (CER)** is calculated by dividing accuracy by cost, which can be formulated as,

$$\mathbf{CER} = \frac{\text{Grid Accuracy}}{\text{Cost}}, \text{ e.g. } (1 \times 1 \text{ Acc.}) / (1 \times 1 \text{ Cost}). \quad (3)$$

A higher score indicates achieving higher accuracy or lower cost. This metric aids in determining the value of utilizing an $n \times n$ grid and deciding which type of $n \times n$ grid to use.

⁵ <https://platform.openai.com/docs/guides/vision>

Table 2: Cost and top-1 accuracy of using collage prompt in GPT-4V’s image recognition. Cost is the overall expense for evaluating 1,000 images. ‘R’ denotes using random arrangements within collage prompt.

Grid Size	1×1		2×2			3×3		
	Cost	Acc.	Cost	Acc.(R)	Acc.(LCP)	Cost	Acc.(R)	Acc.(LCP)
ImageNet-1K	51.30	62.0%	12.83	39.4%	45.7%	5.70	28.1%	33.7%
Caltech101	7.24	95.5%	1.81	88.4%	90.8%	0.80	79.1%	85.4%
OxfordPets	4.99	92.6%	1.25	70.1%	71.8%	0.55	53.2%	59.5%
StanfordCars	21.0	58.3%	5.28	29.8%	32.0%	2.34	11.6%	14.7%
Flowers102	8.58	70.6%	2.15	49.8%	51.1%	0.95	38.4%	43.8%
Food101	8.09	80.1%	2.02	62.2%	64.2%	0.90	39.9%	46.8%
Aircraft	8.61	36.0%	2.15	18.5%	17.7%	0.96	7.0%	10.3%
SUN397	21.55	57.7%	5.39	46.5%	48.7%	2.39	27.6%	36.3%
DTD	5.07	59.1%	1.27	48.6%	52.0%	0.56	37.5%	44.1%
EuroSAT	3.45	36.2%	0.86	42.9%	53.4%	0.38	30.4%	39.7%
UCF101	8.22	51.6%	2.06	55.2%	58.1%	0.91	37.9%	44.0%

- **Precision-Cost Efficiency (PCE)** signifies the money saved per accuracy loss. Its formula is,

$$\text{PCE} = \frac{\text{Cost Saved}}{\text{Accuracy Lost}} = \frac{n \times n \text{Cost} - 1 \times 1 \text{Cost}}{n \times n \text{Acc.} - 1 \times 1 \text{Acc.}} \quad (4)$$

This metric directly reflects the amount of money saved for each point of accuracy lost, balancing accuracy and cost to help choose which type of $n \times n$ grid to use. The goal is to minimize accuracy loss while saving more on costs.

4.4 Results of Collage Prompting

Our analysis reveals that utilizing Collage Prompting with GPT-4V for image recognition significantly reduces inference costs without substantially compromising accuracy as shown in Table 2. By employing low-resolution settings and optimizing image arrangements within collages, we demonstrated that larger grid sizes (2×2 and 3×3) considerably decrease usage costs—approximately to 1/4 and 1/9 of the cost for single images, respectively. Despite a decrease in Top-1 accuracy as grid size increases, our optimized arrangements for these collages effectively minimize accuracy loss, achieving up to 10% higher accuracy over random arrangements across various datasets. This approach highlights the balance between cost efficiency and performance preservation, making it a practical solution for leveraging large multi-modal models like GPT-4V in resource-constrained scenarios.

Our analysis demonstrates the effectiveness of Collage Prompting in enhancing cost-efficiency across various datasets, with $n \times n$ grid collages significantly outperforming single 1×1 images in terms of the Cost-Effective Ratio (CER) as

Table 3: Cost-Effective Ratio (CER) of collage prompt in GPT-4V’s image recognition across diverse datasets.

Grid Size	1×1	2×2		3×3	
	CER	CER(R)	CER(LCP)	CER(R)	CER(LCP)
ImageNet-1K	1.21	3.07	3.56	4.93	5.91
Caltech101	13.19	48.84	50.17	98.33	106.16
OxfordPets	18.56	56.19	57.56	95.95	107.31
StanfordCars	2.76	5.65	6.07	4.95	6.27
Flowers102	8.23	23.22	23.82	40.28	45.94
Food101	9.90	30.75	31.74	44.39	52.06
Aircraft	4.18	8.59	8.22	7.32	10.77
SUN397	2.68	8.63	9.04	11.53	15.16
DTD	11.66	38.34	41.03	66.57	78.28
EuroSAT	10.49	49.74	61.91	79.30	103.57
UCF101	9.93	26.86	28.27	41.50	48.18

Table 4: Precision-Cost Efficiency (PCE) of collage prompt in GPT-4V’s image recognition across diverse datasets.

Grid Size	2×2		3×3	
	PCE(R)	PCE(LCP)	PCE(R)	PCE(LCP)
ImageNet-1K	1.70	2.36	1.35	1.61
Caltech101	0.76	1.16	0.39	0.64
OxfordPets	0.17	0.18	0.11	0.13
StanfordCars	0.56	0.60	0.40	0.43
Flowers102	0.31	0.33	0.24	0.28
Food101	0.34	0.38	0.18	0.22
Aircraft	0.37	0.35	0.26	0.30
SUN397	1.44	1.80	0.64	0.90
DTD	0.36	0.54	0.21	0.30
EuroSAT	-0.39	-0.15	0.53	-0.88
UCF101	0.23	0.26	0.17	0.19

shown in Table 3. The 3×3 grids, optimized through our collage graph optimization method, show the most notable improvements in cost efficiency, especially in datasets with simpler, easily recognizable images. Additionally, our Precision-Cost Efficiency (PCE) analysis underscores the trade-off between cost savings and accuracy loss, highlighting that our optimized 2×2 and 3×3 grid arrangements achieve substantial cost savings while minimizing accuracy loss as shown in Table 4, thereby offering a balanced approach to cost-efficient image recognition with GPT-4V. Unexpected findings, such as the higher-than-anticipated accuracies for 2×2 and 3×3 grids in certain datasets, point to intriguing avenues for future research. Overall, these results underscore the practicality and

Table 5: Evaluation Cost of different methods in ImageNet-1K.

Datasets	Epochs	Accuracy	Training Cost	Test Cost	Total Cost	CER
ViT-B/16	300	84.53%	\$3,876.69	\$32.77	\$3,909.46	0.022
ResNet-50	200	79.04%	\$3,063.99	\$27.64	\$2,091.63	0.038
1×1 Grid	-	62.0%	-	\$641.25	\$641.25	0.097
2×2 Grid	-	45.7%	\$9.9	\$160.37	\$170.27	0.268
3×3 Grid	-	33.7%	\$16.5	\$ 71.25	\$87.75	0.384

efficiency of collage prompting in leveraging large multi-modal models for image recognition tasks under budget constraints.

Cost Analysis and Comparison We estimated the training and inference costs on the ImageNet-1k dataset for CNN and ViT models using AWS cloud servers. We compared the performance of CNNs, ViTs, and collage prompting with GPT-4V in terms of accuracy, cost, and Cost-Effective Ratio (CER). As shown in Table 5, the total costs for training ResNet-50 and ViT-B/16 from scratch amounted to \$2,091.63 and \$3,909.46, respectively. Conversely, employing GPT-4V for single 1×1 image prediction incurred only \$641.25. Remarkably, leveraging collage prompting with 2×2 or 3×3 grid configurations substantially reduced the costs to \$170.27 and \$87.75, respectively.

In terms of the Cost-Effective Ratio (CER), the disparity between collage prompting and traditional CNN and ViT models is stark. For instance, the CER for the 3×3 grid is 17 times higher than that of ViT-B/16, underscoring the cost efficiency of collage prompting compared to conventional training approaches.

4.5 Ablation Study

Cost-Efficiency Analysis of Collage Sizes Table 6 illustrates the Top-1 accuracy of collage sizes ranging from 1×1 to 5×5 random grid arrangements. It also presents the inference time per image and the associated cost of using the GPT-4V API for inference per 1000 images. Notably, transitioning from single 1×1 images to 2×2 grid collages results in a reduction in accuracy of approximately 22.6%. However, the inference time and API usage cost decrease by nearly fourfold. Subsequently, each increment in grid size, from 2×2 to 5×5 , leads to a decrement in accuracy by nearly 10%. Given the impracticality of using 4×4 and 5×5 grid sizes due to their significantly lower accuracy and the extensive search space for grid arrangements, focusing on optimizing the arrangement learning solely for 2×2 and 3×3 grids holds practical value. This is because 2×2 and 3×3 grids maintain acceptable accuracy levels while ensuring sufficiently low costs.

Comparison of Optimization Methods Table 7 compares the efficacy of random initialization, brute force search using a trained model predictor, and

Table 6: Top-1 accuracy, inference time and cost of collage prompts initialization Approaches, Brute Force Solution, and our with different number of images K LCP algorithm for 2×2 and 3×3 Grid Collages. in GPT-4V’s image recognition.

K	Top-1 Acc	Time	Cost	K	Method	Steps	Time	Accuracy
				3×3	Random Init.	-	-	28.1%
1×1	62.0%	8.15s	\$51.30		Brute Force	1,500	9.856	32.8%
2×2	39.4%	2.75s	\$12.83		LCP	500	4.479	33.7%
3×3	28.1%	1.34s	\$5.70		Random Init.	-	-	39.4%
4×4	21.5%	1.05s	\$3.21	2×2	Brute Force	24	0.164	45.1%
5×5	11.9%	0.95s	\$2.05		LCP	9	0.107	45.7%

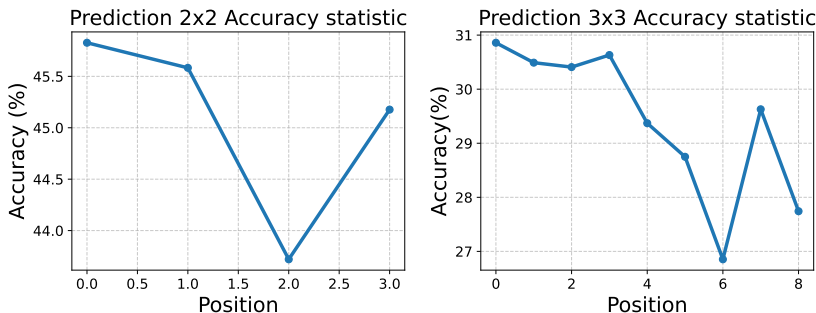


Fig. 4: Average Prediction Accuracy by Position in 2×2 and 3×3 Grids.

optimization using our LCP algorithm for obtaining optimal grid arrangements for both 2×2 and 3×3 collage sizes. It is evident from the table that grid arrangements obtained through the model predictor-based search and optimization generally outperform those obtained through random initialization.

Moreover, the grid arrangements optimized using the LCP algorithm demonstrate higher accuracy levels while requiring fewer steps and less time compared to brute force search. For instance, the LCP algorithm for 3×3 grids achieves a similar accuracy as brute force search but with only 500 steps, three times fewer than brute force, and in half the time. This emphasizes the efficiency and effectiveness of using LCP algorithms for optimizing grid arrangements.

4.6 Case Study

The position statistics depicted in Figure 4 reveal variations in prediction accuracy across different positions within 2×2 and 3×3 grids. Notably, images positioned in the top-left corner exhibit the highest probability of correct predictions, whereas those positioned in the bottom-left corner demonstrate the lowest accuracy. For example, a “room divider” is more accurately recognized when placed in the top-left, as opposed to being mislabeled as a “bed” in other positions. Similarly, “wombat” and “guacamole” samples, considered easier, maintain high accuracy regardless of placement, except when positioned in the least accurate

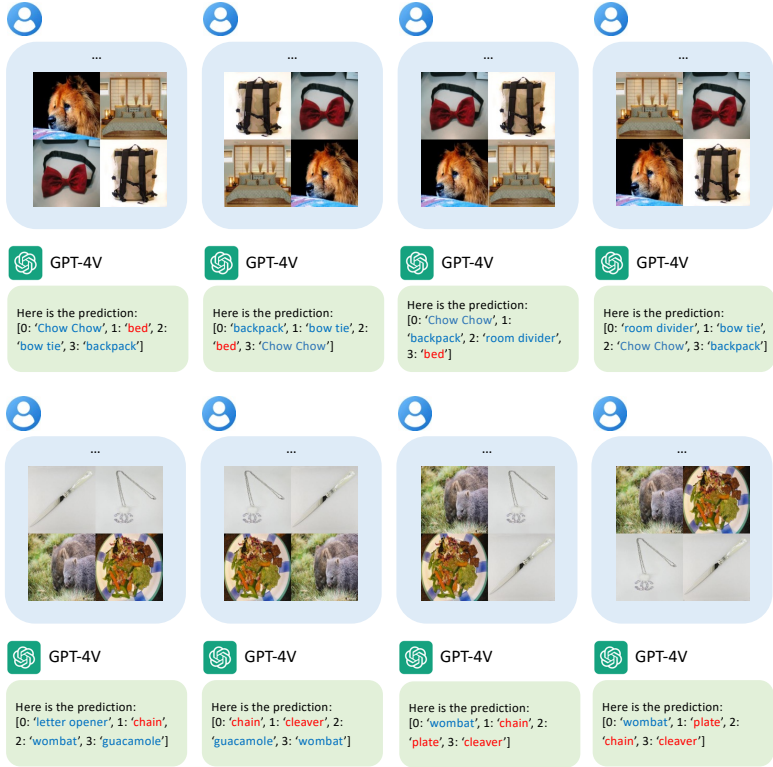


Fig. 5: Case visualization.

bottom-left, which even led to a misprediction of the “guacamole.” This pattern is further exemplified by “letter opener” and “necklace” examples. These findings emphasize the importance of considering spatial arrangement when employing collage prompting in image recognition tasks, suggesting that optimal placement of images can substantially influence the GPT-4V model’s performance.

5 Conclusion

In conclusion, our study introduces Collage Prompting as a novel and cost-efficient method for leveraging GPT-4V in image recognition tasks, demonstrating that optimized image arrangements significantly enhance accuracy while reducing inference costs. Through extensive experimentation, we highlight the advantages of our approach over traditional methods, offering a practical solution to the high costs associated with large multi-modal models. This work not only advances the field of visual recognition but also sets the stage for future research into cost-effective inference strategies for advanced AI models.

References

1. Bahng, H., Jahanian, A., Sankaranarayanan, S., Isola, P.: Exploring visual prompts for adapting large-scale models. arXiv preprint arXiv:2203.17274 (2022) [4](#)
2. Bossard, L., Guillaumin, M., Van Gool, L.: Food-101—mining discriminative components with random forests. In: Computer Vision—ECCV 2014: 13th European Conference, Zurich, Switzerland, September 6–12, 2014, Proceedings, Part VI 13. pp. 446–461. Springer (2014) [8](#)
3. Brown, T., Mann, B., Ryder, N., Subbiah, M., Kaplan, J.D., Dhariwal, P., Nee-lakantan, A., Shyam, P., Sastry, G., Askell, A., et al.: Language models are few-shot learners. *Advances in neural information processing systems* **33**, 1877–1901 (2020) [1](#)
4. Chang, Y., Wang, X., Wang, J., Wu, Y., Yang, L., Zhu, K., Chen, H., Yi, X., Wang, C., Wang, Y., et al.: A survey on evaluation of large language models. *ACM Transactions on Intelligent Systems and Technology* (2023) [1](#)
5. Chen, B., Zhang, Z., Langrené, N., Zhu, S.: Unleashing the potential of prompt engineering in large language models: a comprehensive review. arXiv preprint arXiv:2310.14735 (2023) [4](#)
6. Cheng, Z., Kasai, J., Yu, T.: Batch prompting: Efficient inference with large language model apis. arXiv preprint arXiv:2301.08721 (2023) [4](#)
7. Cimpoi, M., Maji, S., Kokkinos, I., Mohamed, S., Vedaldi, A.: Describing textures in the wild. In: Proceedings of the IEEE conference on computer vision and pattern recognition. pp. 3606–3613 (2014) [8](#)
8. Cui, C., Ma, Y., Cao, X., Ye, W., Zhou, Y., Liang, K., Chen, J., Lu, J., Yang, Z., Liao, K.D., et al.: A survey on multimodal large language models for autonomous driving. In: Proceedings of the IEEE/CVF Winter Conference on Applications of Computer Vision. pp. 958–979 (2024) [3](#)
9. Deng, J., Heybati, K., Shamma-Toma, M.: When vision meets reality: Exploring the clinical applicability of gpt-4 with vision (2024) [3](#)
10. Dosovitskiy, A., Beyer, L., Kolesnikov, A., Weissenborn, D., Zhai, X., Unterthiner, T., Dehghani, M., Minderer, M., Heigold, G., Gelly, S., et al.: An image is worth 16x16 words: Transformers for image recognition at scale. arXiv preprint arXiv:2010.11929 (2020) [2](#)
11. Fei-Fei, L., Fergus, R., Perona, P.: Learning generative visual models from few training examples: An incremental bayesian approach tested on 101 object categories. In: 2004 conference on computer vision and pattern recognition workshop. pp. 178–178. IEEE (2004) [8](#)
12. Han, W., Guo, D., Xu, C.Z., Shen, J.: Dme-driver: Integrating human decision logic and 3d scene perception in autonomous driving. arXiv preprint arXiv:2401.03641 (2024) [3](#)
13. Helber, P., Bischke, B., Dengel, A., Borth, D.: Eurosat: A novel dataset and deep learning benchmark for land use and land cover classification. *IEEE Journal of Selected Topics in Applied Earth Observations and Remote Sensing* **12**(7), 2217–2226 (2019) [8](#)
14. Hu, Y., Lin, F., Zhang, T., Yi, L., Gao, Y.: Look before you leap: Unveiling the power of gpt-4v in robotic vision-language planning. arXiv preprint arXiv:2311.17842 (2023) [3](#)
15. Krause, J., Stark, M., Deng, J., Fei-Fei, L.: 3d object representations for fine-grained categorization. In: Proceedings of the IEEE international conference on computer vision workshops. pp. 554–561 (2013) [8](#)

16. Li, Y., Liu, Y., Wang, Z., Liang, X., Liu, L., Wang, L., Cui, L., Tu, Z., Wang, L., Zhou, L.: A comprehensive study of gpt-4v’s multimodal capabilities in medical imaging. medRxiv pp. 2023–11 (2023) **1**
17. Lin, K., Ahmed, F., Li, L., Lin, C.C., Azarnasab, E., Yang, Z., Wang, J., Liang, L., Liu, Z., Lu, Y., et al.: Mm-vid: Advancing video understanding with gpt-4v (ision). arXiv preprint arXiv:2310.19773 (2023) **1, 3**
18. Liu, P., Yuan, W., Fu, J., Jiang, Z., Hayashi, H., Neubig, G.: Pre-train, prompt, and predict: A systematic survey of prompting methods in natural language processing. ACM Computing Surveys **55**(9), 1–35 (2023) **4**
19. Maji, S., Rahtu, E., Kannala, J., Blaschko, M., Vedaldi, A.: Fine-grained visual classification of aircraft. arXiv preprint arXiv:1306.5151 (2013) **8**
20. Nilsback, M.E., Zisserman, A.: Automated flower classification over a large number of classes. In: 2008 Sixth Indian conference on computer vision, graphics & image processing. pp. 722–729. IEEE (2008) **8**
21. OpenAI: Sora, <https://openai.com/sora> **1**
22. Parkhi, O.M., Vedaldi, A., Zisserman, A., Jawahar, C.: Cats and dogs. In: 2012 IEEE conference on computer vision and pattern recognition. pp. 3498–3505. IEEE (2012) **8**
23. Radford, A., Kim, J.W., Hallacy, C., Ramesh, A., Goh, G., Agarwal, S., Sastry, G., Askell, A., Mishkin, P., Clark, J., et al.: Learning transferable visual models from natural language supervision. In: International conference on machine learning. pp. 8748–8763. PMLR (2021) **5**
24. Radford, A., Wu, J., Child, R., Luan, D., Amodei, D., Sutskever, I., et al.: Language models are unsupervised multitask learners. OpenAI blog **1**(8), 9 (2019) **4**
25. Rombach, R., Blattmann, A., Lorenz, D., Esser, P., Ommer, B.: High-resolution image synthesis with latent diffusion models. In: Proceedings of the IEEE/CVF conference on computer vision and pattern recognition. pp. 10684–10695 (2022) **1**
26. Russakovsky, O., Deng, J., Su, H., Krause, J., Satheesh, S., Ma, S., Huang, Z., Karpathy, A., Khosla, A., Bernstein, M., et al.: Imagenet large scale visual recognition challenge. International journal of computer vision **115**, 211–252 (2015) **2, 6, 8**
27. Shi, Y., Peng, D., Liao, W., Lin, Z., Chen, X., Liu, C., Zhang, Y., Jin, L.: Exploring ocr capabilities of gpt-4v (ision): A quantitative and in-depth evaluation. arXiv preprint arXiv:2310.16809 (2023) **1, 3**
28. Soomro, K., Zamir, A.R., Shah, M.: Ucf101: A dataset of 101 human actions classes from videos in the wild. arXiv preprint arXiv:1212.0402 (2012) **8**
29. Thirunavukarasu, A.J., Ting, D.S.J., Elangovan, K., Gutierrez, L., Tan, T.F., Ting, D.S.W.: Large language models in medicine. Nature medicine **29**(8), 1930–1940 (2023) **1**
30. Tonmoy, S., Zaman, S., Jain, V., Rani, A., Rawte, V., Chadha, A., Das, A.: A comprehensive survey of hallucination mitigation techniques in large language models. arXiv preprint arXiv:2401.01313 (2024) **4**
31. Wake, N., Kanehira, A., Sasabuchi, K., Takamatsu, J., Ikeuchi, K.: Gpt-4v (ision) for robotics: Multimodal task planning from human demonstration. arXiv preprint arXiv:2311.12015 (2023) **3**
32. Wang, J., Wu, Z., Li, Y., Jiang, H., Shu, P., Shi, E., Hu, H., Ma, C., Liu, Y., Wang, X., et al.: Large language models for robotics: Opportunities, challenges, and perspectives. arXiv preprint arXiv:2401.04334 (2024) **3**
33. Wang, Y., Xu, C., Qiu, J., Xu, C., Tao, D.: Towards evolutionary compression. In: Proceedings of the 24th ACM SIGKDD International Conference on Knowledge Discovery & Data Mining. pp. 2476–2485 (2018) **7**

34. Wang, Y., Xu, C., Xu, C., Xu, C., Tao, D.: Learning versatile filters for efficient convolutional neural networks. *Advances in Neural Information Processing Systems* **31** (2018) [2](#)
35. Wen, L., Yang, X., Fu, D., Wang, X., Cai, P., Li, X., Ma, T., Li, Y., Xu, L., Shang, D., et al.: On the road with gpt-4v (ision): Early explorations of visual-language model on autonomous driving. *arXiv preprint arXiv:2311.05332* (2023) [1](#), [3](#)
36. Wu, C., Lei, J., Zheng, Q., Zhao, W., Lin, W., Zhang, X., Zhou, X., Zhao, Z., Zhang, Y., Wang, Y., et al.: Can gpt-4v (ision) serve medical applications? case studies on gpt-4v for multimodal medical diagnosis. *arXiv preprint arXiv:2310.09909* (2023) [3](#)
37. Wu, C., Yin, S., Qi, W., Wang, X., Tang, Z., Duan, N.: Visual chatgpt: Talking, drawing and editing with visual foundation models. *arXiv preprint arXiv:2303.04671* (2023) [4](#)
38. Wu, W., Yao, H., Zhang, M., Song, Y., Ouyang, W., Wang, J.: Gpt4vis: What can gpt-4 do for zero-shot visual recognition? *arXiv preprint arXiv:2311.15732* (2023) [2](#), [3](#), [9](#)
39. Wu, Y., Wang, S., Yang, H., Zheng, T., Zhang, H., Zhao, Y., Qin, B.: An early evaluation of gpt-4v (ision). *arXiv preprint arXiv:2310.16534* (2023) [3](#)
40. Xiao, J., Hays, J., Ehinger, K.A., Oliva, A., Torralba, A.: Sun database: Large-scale scene recognition from abbey to zoo. In: 2010 IEEE computer society conference on computer vision and pattern recognition. pp. 3485–3492. *IEEE* (2010) [8](#)
41. Yang, Z., Li, L., Lin, K., Wang, J., Lin, C.C., Liu, Z., Wang, L.: The dawn of llms: Preliminary explorations with gpt-4v (ision). *arXiv preprint arXiv:2309.17421* **9**(1), 1 (2023) [1](#), [3](#)
42. Yang, Z., Yao, Z., Tasmin, M., Vashisht, P., Jang, W.S., Ouyang, F., Wang, B., Berlowitz, D., Yu, H.: Performance of multimodal gpt-4v on usmle with image: Potential for imaging diagnostic support with explanations. *medRxiv* pp. 2023–10 (2023) [3](#)
43. Zhang, C., Wang, S.: Good at captioning, bad at counting: Benchmarking gpt-4v on earth observation data. *arXiv preprint arXiv:2401.17600* (2024) [3](#)
44. Zhang, Z., Bu, J., Ester, M., Zhang, J., Yao, C., Yu, Z., Wang, C.: Hierarchical graph pooling with structure learning. *arXiv preprint arXiv:1911.05954* (2019) [6](#)
45. Zhao, W.X., Zhou, K., Li, J., Tang, T., Wang, X., Hou, Y., Min, Y., Zhang, B., Zhang, J., Dong, Z., et al.: A survey of large language models. *arXiv preprint arXiv:2303.18223* (2023) [1](#)
46. Zheng, B., Gou, B., Kil, J., Sun, H., Su, Y.: Gpt-4v (ision) is a generalist web agent, if grounded. *arXiv preprint arXiv:2401.01614* (2024) [3](#)
47. Zhou, P., Cao, M., Huang, Y.L., Ye, Q., Zhang, P., Liu, J., Xie, Y., Hua, Y., Kim, J.: Exploring recommendation capabilities of gpt-4v (ision): A preliminary case study. *arXiv preprint arXiv:2311.04199* (2023) [1](#)

A Appendix

A.1 Experimental Details

Network Details. The overall architecture of the collage predictor is depicted in Figure 6. It comprises multiple graph convolutional and pooling layers. The graph convolutional layers aggregate information from neighboring nodes, while the graph pooling layers retain the sub-graph information for each node. This structure preserves the basic graph structural information and facilitates message passing. By learning graph representations hierarchically and summarizing the node representations in each layer using readout functions, the graph representations are then input into a multi-layer perceptron (MLP) to perform graph regression prediction tasks, specifically predicting the overall accuracy of the collage graph.

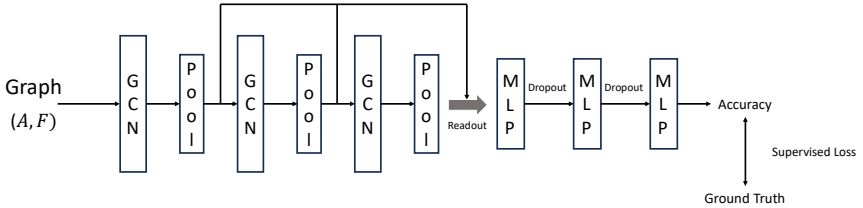


Fig. 6: Network architecture of collage predictor.

Details of Predictor Training. For training the collage predictor, both evaluation datasets for 2×2 and 3×3 collage prompt are split into training and validation sets at a 9:1 ratio, where 90% of the data is allocated for training and the remaining 10% for validation. The collage predictor is trained with a batch size of 512 and a learning rate of 0.001 for 500 epochs. We utilize the Mean Squared Error (MSE) loss function during training. The node input feature dimension of the collage graph network is set to 512. The network architecture consists of three convolutional layers and pooling layers, with a pooling ratio of 0.5. We employ the Adam optimizer to optimize the model. The dimensions of the three MLP layers are set to [256, 128, 64]. During training, we utilize an early stopping strategy to prevent overfitting.

Details of LCP. The pseudocode for our LCP algorithm is provided in Algorithm 1. When predicting arrangements using LCP, we employ uniform crossover without allowing duplicate genes and random mutation to introduce variation in the predicted arrangements for both 2×2 and 3×3 collage prompts. For the 3×3 collage prompt, we initialize the population with 100 arrangements. In each generation, we select the top 20 arrangements with the highest accuracy

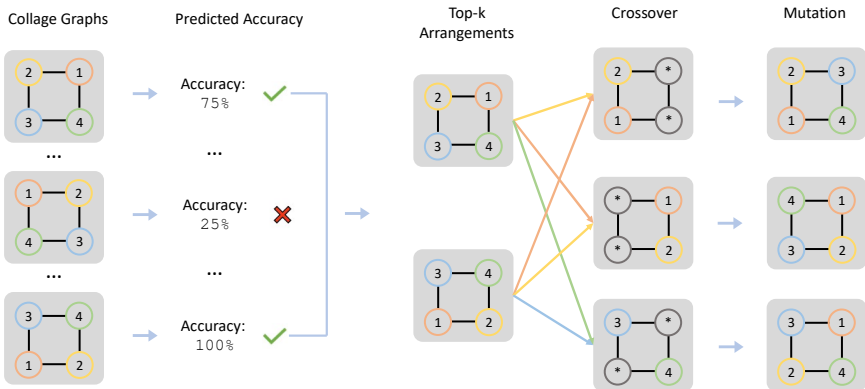


Fig. 7: The process of Crossover and Mutation in the proposed LCP.

to serve as parents for crossover and mutation. The evolution process continues for 10 generations, and we terminate it when the saturation threshold reaches 3. Similarly, for the 2×2 collage prompt, we begin with an initial population of 5 arrangements. We retain the top 3 arrangements in each generation based on accuracy for further reproduction. The evolution process runs for 5 generations, and we stop it when the saturation threshold also reaches 3. Finally, we evaluate the predicted best arrangements by feeding them in batches of 4 to the GPT-4V API to obtain the actual prediction accuracy.

Details of Crossover and Mutation. During the iterative process of optimizing arrangements using LCP, crossover and mutation of arrangements are involved. The specific processes of crossover and mutation are illustrated in Figure 7. At the initial stage of each iteration, our LCP algorithm predicts the accuracy of each initial arrangement using the collage predictor and retains the top-k collage arrangements. Then, any two arrangements from the top-k are randomly selected for node crossover to obtain n partial initial node arrangements for the collages. Finally, the remaining nodes are randomly allocated (mutated) to the blank positions in the collages.

A.2 Additional Visualized Results

The visualization of collage prompt reveals distinct variations in the recognition accuracy of collage images by GPT-4V across different positions within the collage. Specifically, images positioned in the top-left corner exhibit the highest recognition accuracy, while those in the bottom-left corner demonstrate the lowest accuracy. For instance, in the first row of Figure 8, the “Siberian Husky” is misclassified when positioned in the bottom-left corner but correctly identified in other positions. Moreover, relocating challenging samples to the top-left corner

notably enhances GPT-4V’s identification accuracy. For instance, in the second row of Figure 8, the “coffee mug”, identified as a challenging sample, is correctly recognized only when placed in the top-left corner, whereas it is misclassified in other positions. Similarly, such phenomena are observed in the second row of Figure 9.

Algorithm 1: LCP Algorithm for Collage Arrangement Optimization

```

1 Parameters:  $n$ : size of arrangement candidates,  $m$ : size of selected
   arrangement,  $\chi$ : crossover rate,  $\mu$ : mutation rate;
2 Initialise generation 0;
3  $k := 0$ ;
4  $P_k :=$  a set of  $n$  randomly-generated arrangements;
5 Evaluate  $P_k$ ;
6 Compute  $fitness(i)$  for each  $i \in P_k$ ;
7 while not stop-criterion do
8   // Create generation  $k + 1$ ;
9   // 1. Copy;
10  Select Top- $m$  arrangements from  $P_k$ ; insert into  $P_{k+1}$ ;
11  // 2. Crossover;
12  Randomly pop out two arrangements from Top- $m$ ; pair them up;
   produce  $\chi \times n$  new arrangements; insert the arrangements into
    $P_{k+1}$ ;
13  // 3. Mutate;
14  Select  $\mu \times n$  arrangements of  $P_{k+1}$ ; invert a randomly-selected bit in
   each;
15  // Evaluate  $P_{k+1}$ ;
16  Compute  $fitness(i)$  for each  $i \in P_{k+1}$ ;
17  // Increment;
18   $k := k + 1$ ;
19 end
20 return the fittest arrangement from  $P_k$ ;

```

Additionally, we observed instances of mislocalization during collage image recognition by GPT-4V. This phenomenon entails the correct label of an image within the collage being predicted for the adjacent image’s position. For example, in the second row of Figure 8, the “lighthouse” positioned in the bottom-left corner of the third collage is misclassified as the last image in the bottom-right corner. This mislocalization is more pronounced in the first row of Figure 9, where the “projector” is consistently misclassified as a “rotary dial telephone” when adjacent, but correctly classified as other categories when positioned diagonally. This observation offers insight into why the recognition accuracy of images in collages, particularly in datasets like EuroSAT, surpasses that of single images. When images of the same category are juxtaposed in a collage, they provide mutual cues for GPT-4V to predict the correct labels. This phenomenon was further validated through experimentation. These findings underscore the importance of considering the spatial arrangement of images within a collage

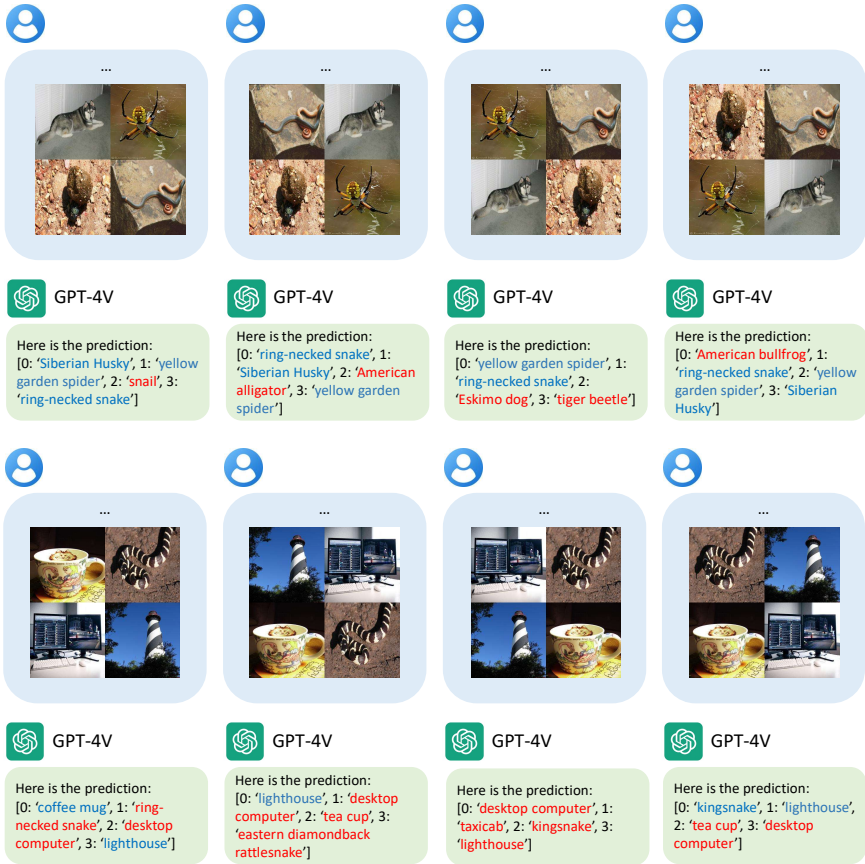


Fig. 8: Two cases that demonstrate different arrangements within the collage prompt lead to different accuracy of classification. Blue indicates an accurate prediction while red indicates a wrong prediction.

when interpreting recognition accuracy and offer insights into the mechanisms underlying GPT-4V's recognition performance in such contexts.

Process of Learning to Collage Figure 10 displays various optimal collage arrangements and their corresponding predictions by GPT-4V across different generations, as generated by the LCP algorithm. In the first row examples, the “automated teller machine” was initially mispredicted in the first two generations but was correctly placed in the top-left corner in the third generation, resulting in a correct prediction by GPT-4V. The optimal arrangement remained consistent in the fourth generation, suggesting that the LCP algorithm stabilized after achieving the best arrangement.

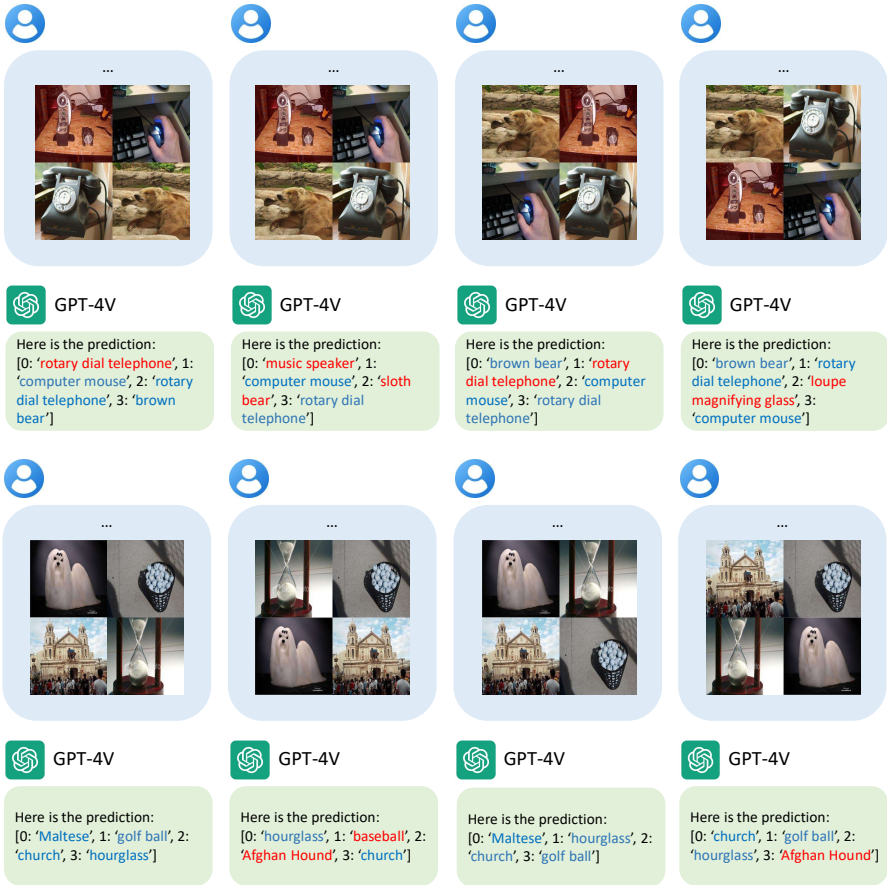


Fig. 9: Two cases that demonstrate different grids within the collage prompt lead to different accuracy of classification. **Blue** indicates an accurate prediction while **red** indicates a wrong prediction.

In the second row examples, the “construction crane” was mispredicted when placed in the bottom-left corner in the first generation. However, it was correctly positioned in the top-left corner in the second generation and remained there in subsequent iterations. This indicates that the LCP algorithm learned to place challenging samples in the top-left corner for improved prediction accuracy, while simpler samples were positioned in the bottom-left corner to enhance overall collage recognition accuracy.

In the third row examples, the “loupe magnifying glass” was initially placed in the bottom-right corner in the first generation, resulting in a misprediction by GPT-4V. Subsequently, in the second generation, the LCP algorithm positioned it in the top-left corner, still leading to a misprediction. However, in the following

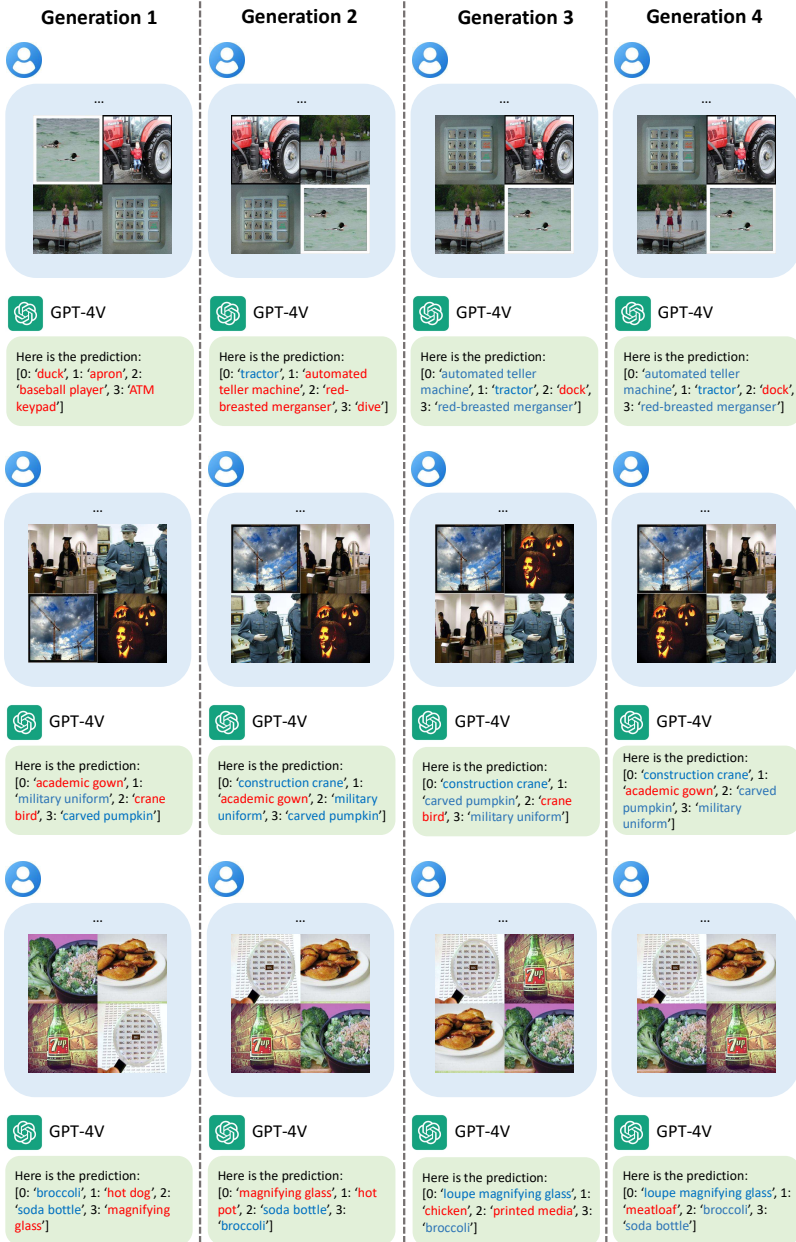


Fig. 10: Illustration of optimized collage arrangements and corresponding GPT-4V predictions across different generations, generated using the LCP algorithm.

iterations, “loupe magnifying glass” persisted in the top-left corner, indicating the LCP predictor’s confidence in this arrangement despite the initial misprediction. Eventually, in the later generations, the correct prediction was made when the “loupe magnifying glass” was placed in the top-left corner again. This example highlights the robustness of our trained LCP predictor and suggests some stochasticity in the prediction outcomes of GPT-4V.

These cases in Figure 10 further demonstrate that GPT-4V’s accuracy in recognizing images within a collage varies across different positions. The LCP algorithm successfully learns the positions that yield the highest and lowest accuracy and optimally arranges the images to enhance the overall collage recognition accuracy by GPT-4V.